

## STUDIES OF HOT B SUBDWARFS. III. CARBON, NITROGEN, AND SILICON ABUNDANCES IN THREE sdB STARS

R. LAMONTAGNE, F. WESEMAEL,<sup>1,2</sup> AND G. FONTAINE<sup>1,2</sup>

Département de Physique and Observatoire du mont Mégantic, Université de Montréal

AND

E. M. SION<sup>1</sup>

Department of Physics, Arizona State University, and Department of Astronomy, Villanova University

Received 1985 April 1; accepted 1985 June 3

### ABSTRACT

Optical and high-dispersion *IUE* observations of three hot B subdwarfs (UV 1758 + 36, Ton S-227, and Feige 65) are presented. These data are analyzed with model atmosphere techniques, and element abundances for C, N, and Si are derived. The abundances are either near (N) or below (C, Si) the solar value; large variations (i) in the extent of underabundances of carbon and silicon among our objects, as well as (ii) in the abundances (with respect to the solar values) characterizing each star are observed. A preliminary interpretation of the observed variations in these and other hot subdwarfs in terms of radiative forces disrupting the downward diffusion of heavy elements is presented.

*Subject headings:* diffusion — stars: abundances — stars: atmospheres — stars: subdwarfs — ultraviolet: spectra

### 1. INTRODUCTION

Any understanding of the evolutionary status of hot subdwarfs and the importance of these objects for the evolution of low- and intermediate-mass stars must provide answers to the two following questions: (1) Are the hot O and B subdwarfs genetically related? If so, what evolutionary phase do they represent? If not, why are some of their properties and characteristics so similar? (2) What are the physical mechanisms that influence the surface composition of hot subdwarfs?

Over the past 10 yr, some clues to the atmospheric properties and evolutionary status of the hot subdwarfs have become available through both theoretical studies of model evolutionary tracks and detailed model atmosphere and abundance analyses of individual objects. In particular, the abundance differences that have been found between various classes of subdwarf stars will, ultimately, have to be interpreted either in terms of different initial conditions, or as a logical consequence of physical processes (such as convective mixing, or element diffusion) operating along a single evolutionary track.

Abundance analyses of hot subdwarfs based on high-dispersion, far-ultraviolet observations from the *International Ultraviolet Explorer* (*IUE*) constitute a powerful tool for the study of these questions; initial studies of high-dispersion spectra of hot subdwarfs have underscored the usefulness of such observations by revealing an ultraviolet spectrum very rich in metal lines (Baschek, Kudritzki, and Scholz 1980; Gruschinske *et al.* 1980; Simon *et al.* 1980; Bruhweiler, Kondo, and McCluskey 1981; Baschek *et al.* 1982 [BKSS]; Baschek, Höflich, and Scholz 1982 [BHS]; Heber *et al.* 1984a; Lynas-Gray *et al.* 1984; Rossi, Viotti, and Altamore 1984). These investiga-

tions, some of them still in preliminary stages, have already revealed some interesting patterns. Silicon, for example, has been suggested to be in solar abundance in the hot sdO, but strongly deficient in the intermediate-temperature OB subdwarfs. This result is interpreted by BKSS and BHS as the result of a change in the ionization state of the Si atom, which could affect its radiative support. That this explanation is at least reasonable can readily be appreciated from the work of Michaud, Vauclair, and Vauclair (1983), which shows that radiative forces on heavy elements can be large in low-mass horizontal-branch stars. The radiative support would be even more efficient in the hot B subdwarfs, which have comparable gravities but even higher effective temperatures.

In order to further elucidate the potential importance of various physical mechanisms in the photospheres of hot subdwarfs and to study the genetic links between the existing subclasses, we have initiated a study of metal abundance patterns in the hot B subdwarfs. As part of this effort, we have observed three stars, UV 1758 + 36, Ton S-227 (PHL 1126, FB 19, SB 707, GD 1391, CD - 24°731), and Feige 65 (PG 1233 + 426, FB 101), with the *IUE* satellite in the high-dispersion mode.<sup>3</sup> These three objects, with effective temperatures ranging from 26,000 to 34,000 K cover a domain not sampled in earlier abundance studies of hot, hydrogen-rich subdwarfs. Their analysis, together with existing abundance determinations in several other sdOB and sdO stars, is expected to provide quantitative information on the element abundance patterns on the so-called extended horizontal branch (Greenstein and Sargent 1974).

In what follows, we first present our *IUE* and optical data,

<sup>1</sup> Guest Investigator with the *International Ultraviolet Explorer* satellite, which is sponsored and operated by the National Aeronautic and Space Administration, by the Science Research Council of the United Kingdom, and by the European Space Agency.

<sup>2</sup> Visiting Astronomer, Kitt Peak National Observatory, National Optical Astronomy Observatories, which is operated by AURA, Inc., under contract with the National Science Foundation.

<sup>3</sup> In Heber *et al.* (1984b), Ton S-227 is described as a sdOB star, presumably because of its relatively high effective temperature ( $T_e = 34,000$  K). We prefer to reserve the sdOB (or, perhaps more appropriately, the sdBO) appellation to those hydrogen-rich stars which do show He II  $\lambda 4686$  (such as Feige 66, HD 149382, and Feige 110). Ton S-227 has no reported  $\lambda 4686$  feature (Greenstein and Sargent 1974; Heber *et al.* 1984b), and that line is, at best, weak in our own spectra; we thus adopt the sdB classification for that object.

TABLE 1  
IUE HIGH-DISPERSION OBSERVATIONS

Target	Image Number	$t_{\text{exp}}$ (minutes)
UV 1758 + 36 .....	SWP 20668	225
Ton S-227 .....	SWP 20337 <sup>a</sup>	240
	SWP 21362	210
Feige 65 .....	SWP 21373	300

<sup>a</sup> Data drop during image transmission.

together with the various methods of reduction and analysis used (§ II). In § III, we describe the model calculations used to determine the metal abundances in our program objects. The results of these analyses are then presented and discussed in § IV. Finally we offer, in § V, some comments on the astrophysical implications of our results, and on how they relate to previous abundance determinations in hot subdwarfs.

## II. OBSERVATIONS AND DATA REDUCTION AND ANALYSIS

### a) The IUE Spectra

High-dispersion IUE spectra of our three program objects were obtained with the SWP camera in 1983. The image numbers and exposure times are provided in Table 1. Because our target stars were all relatively faint for high-dispersion work ( $y = 11.37, 11.76, \text{ and } 12.04$  for UV 1758 + 36, Ton S-227, and Feige 65, respectively), all our images were underexposed.

Radial velocities were determined for our three target stars on the basis of the measured velocity shifts of the strongest among the C III, C IV, N III, N IV, and N V features. Typically, 12 lines were used to determine the radial velocity. These results are summarized in Table 2, where we also list previous radial velocity measurements. The agreement with these earlier values is fair. In UV 1758 + 36, the stellar radial velocity is such that a complete separation of photospheric and interstellar components was never possible. This problem was compounded by the fact that the interstellar lines display an unexpectedly large shift of their own; we measure  $v_{\text{ISM}} = -43 \pm 1 \text{ km s}^{-1}$  on that line of sight, based on the identification of C II, N I, Si II, and S II features. Ton S-227 and Feige 65 are better suited to attempts to separate the stellar from the interstellar components, but this procedure has been greatly complicated by the intrinsic noise level in our spectra and, thus, has proved only mildly successful. Finally, we found no evidence for P Cygni profiles (e.g., Hamann *et al.* 1981) or for line velocity structure (e.g., Bruhweiler and Dean 1983; Bruhweiler 1984) in any of our spectra.

TABLE 2  
SUMMARY OF RADIAL VELOCITIES

STAR	$v_r$ (km s <sup>-1</sup> )	
	This Work	Other Studies
UV 1758 + 36 .....	$-51 \pm 1$	$-38 \pm 10^a$
Ton S-227 .....	$+73 \pm 2$	$+49^b \pm 2, +101^c, +61 \pm 50^d$
Feige 65 .....	$+36 \pm 3$	$+55^c$

<sup>a</sup> Giddings and Dworetzky 1978.

<sup>b</sup> Graham and Slettebak 1973.

<sup>c</sup> Greenstein and Sargent 1974.

<sup>d</sup> Heber *et al.* 1984b.

### b) The Optical Spectra

Optical spectrophotometric observations were also obtained in order to determine surface gravities. Feige 65 and UV 1758 + 36 were observed on 1984 April 8 and 9 (UT), and Ton S-227 on 1984 August 11 (UT), with the IIDS system behind the "gold" spectograph attached to the Kitt Peak National Observatory 2.1 m reflector. The total integration times were 10, 10, and 14 minutes for Feige 65, UV 1758 + 36 and Ton S-227, respectively. The 600 lines mm<sup>-1</sup> grating (No. 35) was used in second order, and provided coverage of the 4050–5000 Å region. An entrance aperture of 6" was used, and the resulting spectral resolution was better than 4.25 Å. Surface gravities determined from the H $\beta$  and H $\gamma$  line profiles are obtained in § IIIa.

### c) Method of Analysis of the IUE Images

Because of the numerous absorption lines expected in the far-ultraviolet spectra of hot subdwarfs, and of the intrinsic noise level in our high-dispersion images, there seems to be no truly objective way to set the continuum level in our spectra. After different attempts, the procedure we have adopted consists of fitting a spline through each individual (and previously smoothed) spectral order, using typically from 10 to 15 visually chosen points per order to define collocation points. The resulting continuum was used to measure equivalent widths. In order to gain some understanding of the systematic errors inherent to different continuum setting procedures, we have used our method to measure equivalent widths of several lines in the high-dispersion images of the sdOB stars HD 149382 (SWP 5193) and Feige 66 (SWP 14567); these images were obtained from the Astronomical Data Center, and were analyzed in detail by BKSS and BHS, respectively. A comparison of their published equivalent widths with our own measurements shows average differences of  $\sim 20\%$ —with our widths being generally, but not consistently, lower than theirs. Some of that difference is undoubtedly due to our correcting in an approximate manner for the improper background subtraction due to order overlap at the short-wavelength ( $\lambda \lesssim 1500 \text{ \AA}$ ) end of the SWP camera (see § II d), while Baschek and collaborators preferred the standard IUE background correction procedure.

Another check on the consistency of our procedure was provided by the use of an earlier image of Ton S-227 (SWP 20337). Although its usefulness for abundance determinations is limited because of a data drop during transmission, this image permits an independent measurement of the width of selected lines. The measured equivalent widths reproduced within 15%–20% on the average.

Our line identifications were made by comparing the velocity-corrected wavelength of observed features with those tabulated in Kelly and Palumbo (1973). In general, a wavelength agreement of 0.1 Å between laboratory and measured values was required for identification. Because of the intrinsic noise level in our spectra, we have restricted the data presented and analyzed here to photospheric features associated with the astrophysically important (and abundant) ions of C, N, and Si. For those ions, our identifications were cross-checked against those of BKSS and BHS in the bright sdOB stars HD 149382 and Feige 66. The lines of these three ions identified in our program stars, and their equivalent widths, are listed in Table 3. In addition, we have also tentatively identified features associated with various ionization states of the following elements on our best image, that of UV 1758 + 36 (SWP 20668):

TABLE 3  
LINE IDENTIFICATIONS AND EQUIVALENT WIDTHS

ION	$\lambda_{\text{lab}}$	$\chi$ (eV)	$W_{\lambda}$ (mÅ)		
			UV 1758+36	Ton S-227	Feige 65
C II	1323.91/3.95	9.3	110	41	168
	1335.70	0.0	187	51:	320
C III	1174.-1176. <sup>a</sup>	6.5	940	384	1217
	1247.38	12.7	130	<20	180:
	1531.85	32.1	104:	<79	134:
	1620.05	32.2	...	...	42
	1922.93/3.14	33.5	108	163:	<199
C IV	1548.20	0.0	209:	23	225
	1550.77	0.0	231	<207	139:
N III	1183.03	18.1	115	118	130
	1184.54	18.1	136	98	160
	1387.37	30.5	<134	<186	<62
	1729.94	41.0	...	61:	...
	1747.86	18.1	145	118	36:
	1751.24/1.75	18.1	150	333	280:
	1804.3/4.5	41.3	60:	114:	116:
	1805.66	30.5	53:	74:	...
	1845.71/5.86	41.3	...	41	66:
	1846.41	41.3	...	...	...
1885.25	33.2	85	166:	<114	
N IV	1718.55	16.2	91	<148	...
N V	1238.82	0.0	43	73	<58
	1242.80	0.0	<60	94	28
Si II	1190.42	0.0	...	...	79:
	1260.42	0.0	...	...	<202
	1264.74	0.0	...	...	39:
	1304.37	0.0	...	...	<24
Si III	1206.51/6.53	10.3	...	...	345:
	1301.15	6.6	...	...	123
	1303.32	6.6	...	...	117
Si IV	1393.75	0.0	<20	<20	516
	1402.76	0.0	<20	<20	374

<sup>a</sup> Six components at  $\lambda = 1174.93, 1175.26, 1175.59, 1175.71, 1175.99, 1176.37$  Å.

Ne, Mg, Al, P, S, Ar, Ca, Sc, Ti, V, Cr, Mn, and Fe. However, confirmation of these preliminary identification and abundance analyses for the heavier metallic ions, such as those performed in the exhaustive investigations of BKSS and BHS, must await additional *IUE* images with increased exposure levels.

#### d) *IUE* Background Correction Procedures

It is a well-known problem that the decreasing spacing between echelle orders at the short-wavelength end of the SWP camera leads to problems in the evaluation of the background level. In the present analysis, we have used the empirical method of Bruhweiler and Kondo (1982) to correct the equivalent widths for the improper background subtraction in our image. For features below  $\sim 1500$  Å, the measured widths were divided by a smoothly varying factor, interpolated from the values provided by Bruhweiler and Kondo (1982).

After much of our analysis was completed, we became aware of a recent paper by Bianchi and Bohlin (1984), where a method is devised to correct the net *IUE* spectra for order overlap. As a test of our overlap-correction scheme, we implemented the Bianchi and Bohlin procedure and performed some spot-checking of its results. We found differences between the widths obtained from the two procedures occasionally as large as  $\sim 20\%$ , but on the average of only  $\sim 5\%$ . Hence, we feel

that our empirical correction procedure is entirely adequate for the widths measurements presented here.

### III. ATMOSPHERIC PARAMETERS AND METHOD OF ANALYSIS

#### a) *Atmospheric Parameters*

Before proceeding with our planned abundance analyses, we must first obtain effective temperatures and surface gravities for our program objects. The effective temperature is obtained by fitting the composite (optical and ultraviolet) energy distribution with fluxes determined from model atmosphere calculations. The gravity is then determined through fits to the Balmer line profiles. As helium is always deficient in the B subdwarfs, the exact helium abundance is inconsequential for the determinations of  $T_e$  and  $\log g$ , as well as for that of the heavy elements.

For UV 1758+36, we have used the effective temperature recently determined for that object,  $T_e = 31,800 \pm 1100$  K, a result based on the analysis of *Voyager* far-ultraviolet spectrophotometry (Wesemael *et al.* 1985). The surface gravity was then determined by fitting the H $\beta$  and H $\gamma$  profiles. Our line profile fits yield  $\log g = 5.6 \pm 0.3$ ; these results are displayed in Figure 1. Earlier, Giddings and Dworetzky (1978) had presented a model atmosphere analysis of UV 1758+36 based on intermediate-band photometry and optical spectroscopy.

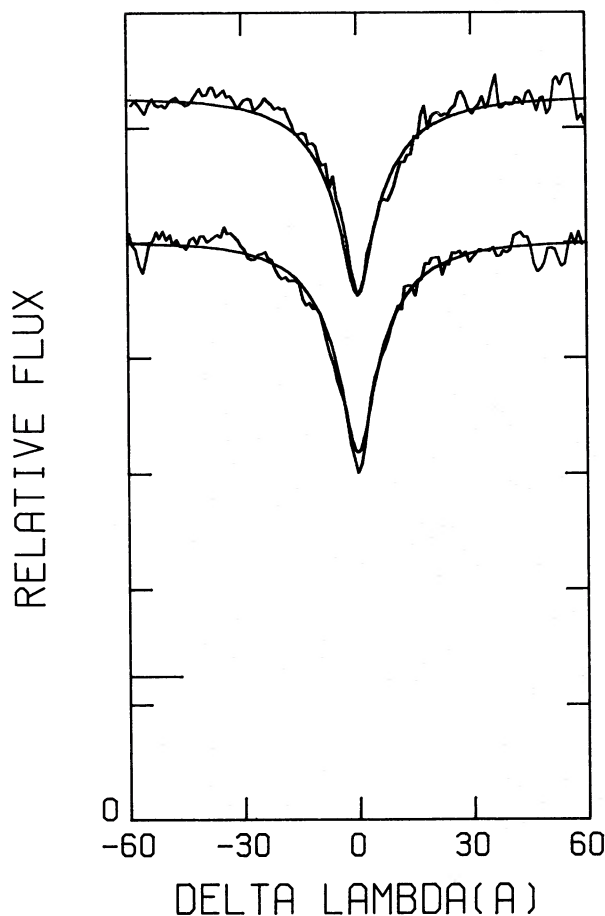


FIG. 1.—Best fits to  $H\beta$  (top) and  $H\gamma$  (bottom) profiles of UV 1758+36. Profiles shown are for  $T_e = 31,800$  K and  $\log g = 5.6$ . Both observed and theoretical profiles have been normalized at  $\pm 60$  Å from line center, and theoretical profiles have been folded with a Gaussian of FWHM = 4.25 Å. Zero-point of lowermost plot is at bottom of figure; that of top plot is indicated by long tick mark.

Their results,  $T_e = 32,500 \pm 2500$  K and  $\log g = 5.25 \pm 0.25$ , are in good agreement with those presented here.

For Ton S-227, we have used the results of Heber *et al.* (1984b),  $T_e = 34,000 \pm 2000$  K,  $\log g = 6.0 \pm 0.3$ , based on analyses of *IUE* spectrophotometry and Balmer line profiles.<sup>4</sup> Our fully independent reanalysis of low-dispersion *IUE* and optical spectrophotometry of this object (using similar assumptions—see footnote 4) yields results identical to those of Heber *et al.* (1984b), and thus provides a useful check on both analyses. Because of this agreement, the results of our fits are not displayed here.

For Feige 65, low-dispersion *IUE* images (SWP 21374,  $t_{\text{exp}} = 4$  m; LWP 2149,  $t_{\text{exp}} = 5.5$  m) were combined with the Strömgen photometry of Bergeron *et al.* (1984) to construct

<sup>4</sup> In that analysis, and in that of Feige 65 which follows, the determination of the interstellar reddening is decoupled from the effective temperature determination:  $T_e$  is determined by fitting an *unreddened* energy distribution, and the color excess can then, if necessary, be determined from the optical photometry. While this procedure is not entirely self-consistent, there are serious difficulties in determining simultaneously  $T_e$  and  $E(B-V)$  in lightly reddened objects; indeed, an apparently unreddened energy distribution can often equally well be matched with a slightly (approximately a few thousand degrees) hotter and slightly reddened [ $E(B-V) \lesssim 0.04$ ] model. See Wesemael *et al.* (1985) for further discussions of this point.

the composite energy distribution shown in Figure 2. Our optimal fit to the data, obtained with unreddened, fully blanketed solar-composition models from Kurucz (1979), is achieved at  $T_e = 26,200 \pm 1500$  K, and is also displayed. The Balmer profile fit then yields  $\log g = 5.3 \pm 0.3$ . The resulting fits are displayed in Figure 3.

#### b) Abundance Analysis

Model calculations with the atmospheric parameters summarized above were performed to determine metal abundance in our target stars. The first step in this procedure is the computation of a LTE, hydrogen line blanketed, metal-free model (see, e.g., Wesemael *et al.* 1980). The temperature and density stratifications of this model are then used to compute the appropriate level populations of the various metal ions, which are thus treated as trace elements. Synthetic fluxes over narrow wavelength regions of interest are then recalculated, with the metal line opacity now included. The basic features of the LTE line formation program are described briefly by Henry, Shipman, and Wesemael (1985).

For uniformity, we have adopted most of the radiative damping widths listed by BKSS. Electron (and ion) impact widths for several strong ultraviolet lines were also available (e.g., from Sahal-Bréchet and Segre 1971) and were included. All our oscillator strengths are from Wiese, Smith, and Glennon (1966), except for that of C III  $\lambda 1923$ , which is based on the lifetime measurements of Poulizac, Druetta, and Ceyzériat (1971). Since only a limited number of spectral lines of a given element are measurable on our spectra, we have not determined directly the microturbulent velocity  $\zeta$  appropriate for each object. Rather, we have made use of the results of BKSS and Simon *et al.* (1980), as well as those of Dufton, Durrant, and Durrant (1981), and adopted a constant value  $\zeta = 5$  km  $s^{-1}$  for all three stars. The changes in element abundances brought about by small variations in  $\zeta$  have been investigated by BKSS and BHS, and are further discussed in § IVb.

As a check of the reliability of our abundance determinations, we have reanalyzed most of the carbon, nitrogen, and silicon equivalent widths measured by BKSS and BHS in HD 149382 and Feige 66, respectively. The abundance we determine for individual lines agree generally well with the BKSS and BHS values (i.e., within 0.2–0.3 dex); the largest difference is for the N III  $\lambda 1885.25$  line in Feige 66, where we find (with the lower limit of  $\gamma_{\text{rad}}$  given by BKSS) a difference of 0.6 dex. We emphasize that these results include not only differences due to the different synthetic line profile programs, but also those “built into” the different metal-free atmosphere models at given values of  $T_e$  and  $\log g$ ; in particular, the differences in surface temperature stratifications between the non-LTE models of Baschek and collaborators and our own LTE models may well play some role here.

A final concern is the reliability of LTE line transfer in our abundance determinations. However, test calculations performed by BKSS on C, N, and Si ions suggest no significant departures from LTE in HD 149382; we may expect these results to apply as well to the three cooler stars analyzed here.

### IV. C, N, AND SI ABUNDANCES IN HOT B SUBDWARFS

#### a) Results of Abundance Analyses

The average element abundances obtained for our three program objects are summarized in Table 4. We now discuss briefly the individual determinations for each element.

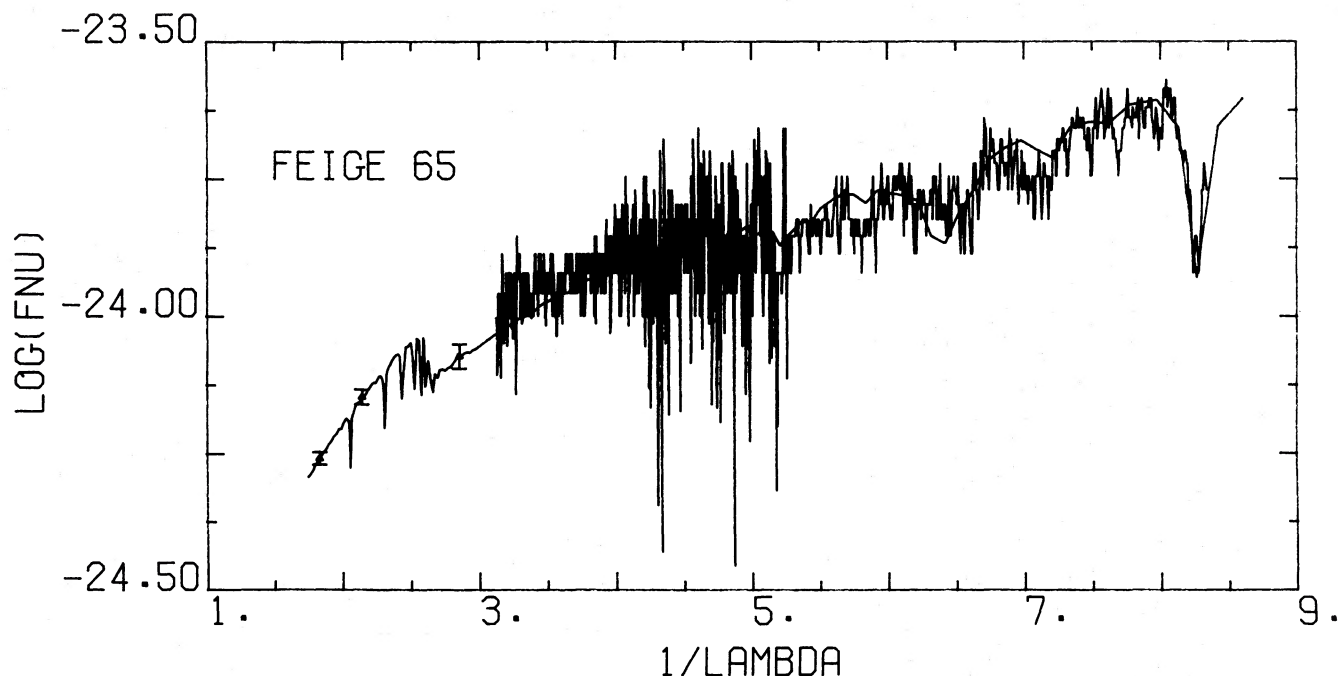


FIG. 2.—Observed combined (Strömgren and IUE) energy distribution of Feige 65, together with optimal model from Kurucz (1979). The Strömgren  $u$ ,  $b$ , and  $y$  magnitudes are represented by three points with associated error bars, and IUE data by solid line. Effective temperature is  $T_e = 26,200$  K.

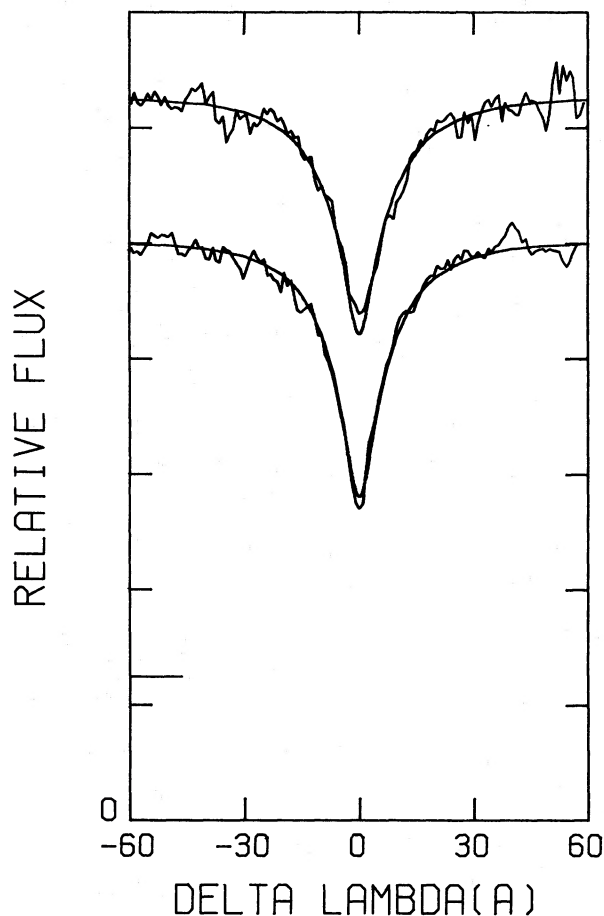


FIG. 3.—Same as Figure 1, but for Feige 65. Profiles displayed are for  $T_e = 26,200$  K and  $\log g = 5.3$ .

#### i) Carbon

We find a greatly variable carbon abundance in our objects, with differences of a factor of  $\sim 1000$  in the carbon contents of Ton S-227 and Feige 65. Our values are, typically, averages based on five lines encompassing three ionization states. We found an occasional tendency for C II  $\lambda 1323.9$  to yield somewhat larger abundances than the other features analyzed. A similar result was also seen in our reanalysis of the BKSS and BHS measurements of that line (see § IIIb).

The region around  $1175 \text{ \AA}$ , which features the prominent C III  $2s2p^3P^o-2p^2^3P$  transition, is displayed in Figure 4a. The same wavelength range in the (brighter) sdOB stars HD 149382 and Feige 66 is displayed in Figure 4b (BKSS, BHS), and typifies the difference in signal-to-noise ratio between both sets of observations.

TABLE 4  
C, N, AND SI ABUNDANCES IN HYDROGEN-RICH HOT SUBDWARFS

STAR	ABUNDANCES <sup>a</sup>			REFERENCE
	$\epsilon_C$	$\epsilon_N$	$\epsilon_{Si}$	
UV 1758 + 36 .....	$6.6 \pm 0.7$	$7.6 \pm 0.6$	$< 2.1$	This work
Ton S-227 .....	$4.2 \pm 1.0$	$8.0 \pm 0.8$	$< 2.2$	This work
Feige 65 .....	$7.3 \pm 0.7$	$8.2 \pm 1.0$	$5.5 \pm 0.8$	This work
HD 149382 .....	$6.6 \pm 0.3$	$8.0 \pm 0.3$	$< 2.3 \pm 0.6$	1
Feige 66 .....	$6.4 \pm 0.3$	$8.2 \pm 0.3$	$< 2.3 \pm 0.6$	2
Feige 110 .....	$\leq 3.0$	7.8	$< 3.8$	3
LB 3459 .....	6.5	...	6.4	4
HD 205805 .....	$\sim 8.5$	$\sim 8.0$	$\sim 7.5$	5
HD 4539 .....	$\sim 8.3$	$\sim 8.5$	$\sim 7.5$	6
Sun .....	8.5	8.0	7.5	...

<sup>a</sup>  $\epsilon_Z = 12 + \log [N(Z)/N(H)]$ .

REFERENCES.—(1) Baschek *et al.* 1982; (2) Baschek, Höflich, and Scholz 1982; (3) Heber *et al.* 1984a; (4) Lynas-Gray *et al.* 1984; (5) Baschek and Norris 1970; (6) Baschek, Sargent, and Searle 1972.

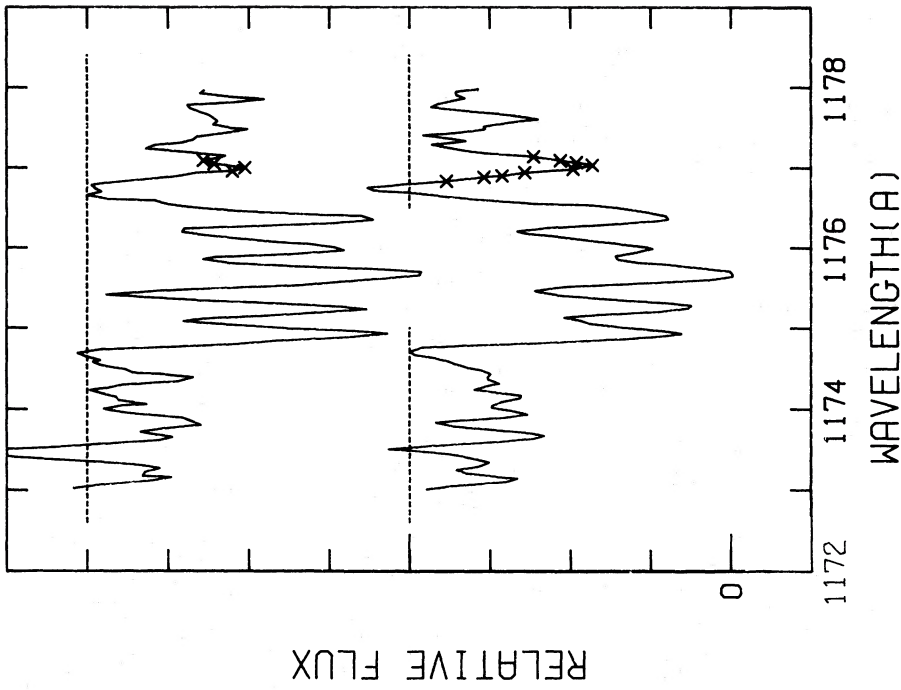
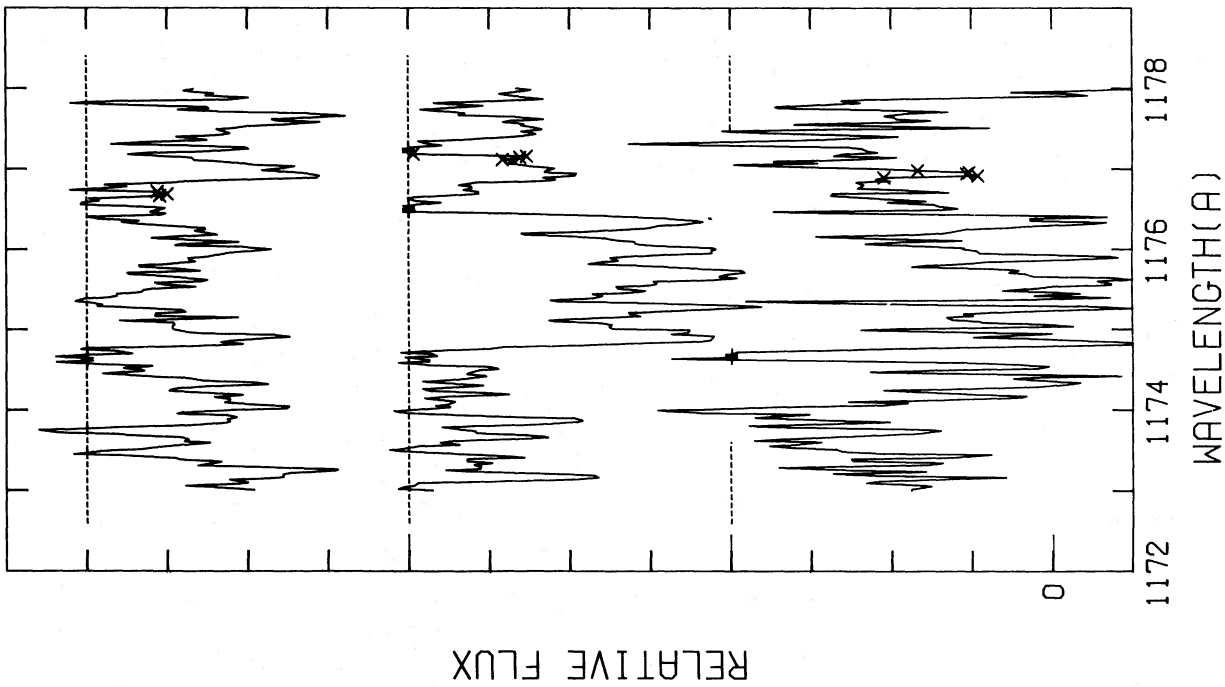


FIG. 4.—(a) Region around 1175 Å in high-dispersion spectra of Ton S-227 (top), UV 1758+36 (center) and Feige 65 (bottom). Feature is the C III  $2s2p^3P^o-2p^2^3P$  transition. Dotted lines indicate approximate continuum level in that spectral region; all three spectra are on laboratory wavelength scale. Zero point for bottom plot is indicated; for upper plots, the two lowermost dotted lines also serve as zero points. Crosses are instrumental resseau marks, (b) same as (a), but for the sdOB stars Feige 66 (top) and HD 149382 (bottom), observed by BHS and BKSS, respectively.



## ii) Nitrogen

In contrast to carbon, nitrogen abundance appears remarkably stable from star to star, with variations of a factor of only  $\sim 4$  in our sample. The abundances given are averages of between five and eight transitions from three different ionization stages.

## iii) Silicon

For two objects, the silicon abundance rests exclusively on the absence of the Si IV resonance lines ( $\lambda\lambda 1393.755, 1402.770$ ), which yields stringent upper limits on the Si/H abundance ratio. However, in the coolest star of our sample, Feige 65, the Si IV resonance lines are seen, as are additional transitions from lower silicon ionization stages. The striking difference in appearance of the region around 1394 Å is displayed in Figure 5 for our program objects; the abundance analysis indeed confirms that Si is enhanced in Feige 65 compared to our two other targets.

## b) Accuracy of Abundance Determinations

Two broad classes of uncertainties affect the abundance values given in Table 4. First, those pertaining to the observational aspects of the abundance analysis, such as the continuum setting procedure, the *IUE* background subtraction, unrecognized atomic blends, blended ISM components, etc. For well-exposed spectra, the measurement of equivalent widths of  $\sim 100$  mÅ should be accurate to better than  $\sim 15\%$ ; this uncertainty may increase, however, in the case of underexposed images, or of difficult continuum setting—clearly the case here. This would lead to uncertainties in the average abundance values of up to  $\sim 0.3$  dex.

Second, uncertainties associated with the theoretical modeling of the observed features also affect the abundance determinations. These include inadequacies in the model atmospheres, and uncertainties in the damping widths, oscillator strengths, and microturbulent velocities. The uncertainties associated with these theoretical ingredients are, for the most part, accounted for by the comparisons discussed in § IIIb (we adopt here a typical uncertainty of  $\pm 0.3$  dex). Not included in these comparisons, however, is the influence of changes in the microturbulent velocity  $\zeta$ . While the importance of  $\zeta$  depends on the location of individual lines on the curve of growth, its influence on the *average* abundances of, e.g., UV 1758 + 36, is to increase the carbon and nitrogen abundance by 0.2–0.3 dex if a value of  $\zeta = 0$  km s $^{-1}$  is adopted instead of  $\zeta = 5$  km s $^{-1}$ . Further details on the influence of  $\zeta$  on *individual* lines can be gathered from the work of BKSS and BHS.

The error estimates listed in Table 4 for our three objects incorporate the uncertainties associated with the three sources discussed here, together with the mean error obtained from averaging the abundances obtained from several individual lines.

## V. ASTROPHYSICAL IMPLICATIONS AND CONCLUDING REMARKS

The abundances determined in our three target stars, augmented by those measured earlier by others in six additional objects of type sdB and sdOB (see Table 4), permit us to identify—perhaps for the first time—some systematic trends in the abundances of hot B and OB subdwarfs. Of these six objects, four have abundances based on high-dispersion *IUE* observations similar to those presented in this paper. Two

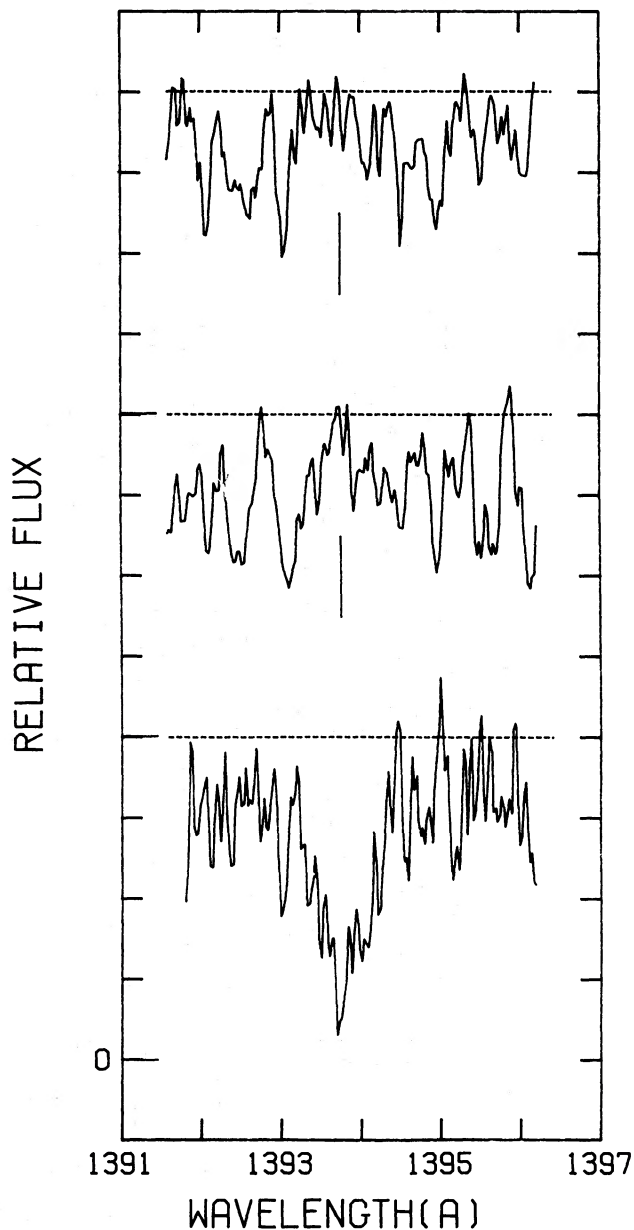


FIG. 5.—Same as Fig. 4a, but for region around Si IV  $\lambda 1393.755$  resonance transition. Feature is absent in Ton S-227 (top) and UV 1758 + 36 (center), and its expected location in these two objects is indicated by long vertical marks.

additional objects have metal abundances estimated or determined from *optical* spectra only. Because hydrogen is their dominant atmospheric constituent, we are inclined to consider these stars as a reasonably homogeneous group, and we collectively refer to them as hydrogen-rich hot subdwarfs.

We present, in Figure 6, a graphical summary of the dependence of the C, N, and Si abundances in these nine hydrogen-rich hot subdwarfs on the effective temperature. The carbon abundance shows large variations, by a factor of  $\sim 10^3$ , from star to star; in all cases, however, carbon is found to be either at, or below, the solar abundance. The data also indicate that the carbon abundance may tend to decrease with increasing effective temperature; however, the interpretation of the

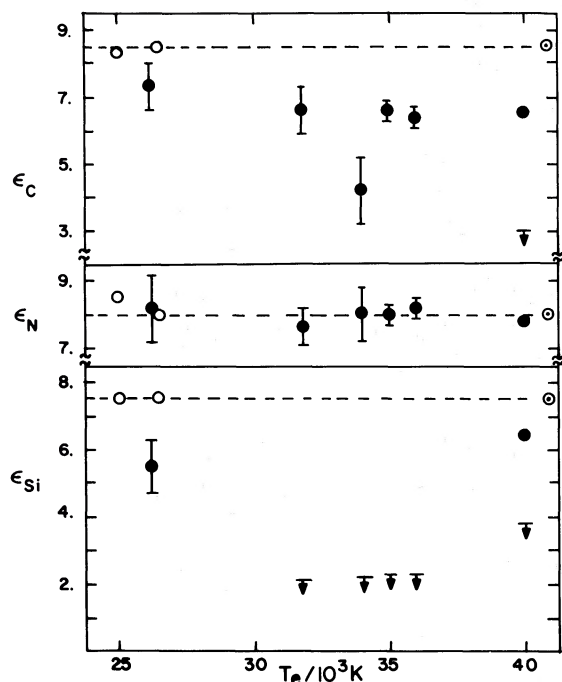


FIG. 6.—Summary of carbon, nitrogen, and silicon abundances determined up to now in hydrogen-rich, hot subdwarfs. Filled circles represent studies based on analysis of high-dispersion *IUE* data. Open circles are those based on optical data (see § V). In all three panels, dashed line—marked “○”—indicates appropriate solar abundance. Individual effective temperatures are, in general, accurate to  $\sim \pm 1500$ – $2000$  K.

behavior of  $\epsilon_C$  at the hot end is muddled by the contrasting carbon abundances measured in Feige 110 ( $\epsilon_C \leq 3.0$ ) and LB 3459 ( $\epsilon_C = 6.5$ ), both at  $T_e = 40,000$  K. In the hot sdO stars, which have either mixed-composition or helium-rich atmospheres, and which prolong the subdwarf temperature sequence above  $\sim 40,000$  K, carbon is also found to be underabundant, but only by a factor  $\lesssim 10$  (Simon *et al.* 1980).

The nitrogen abundance measured in eight hydrogen-rich objects is noteworthy in that it displays essentially no variations over the range 25,000–40,000 K; in addition, the average nitrogen abundance is consistent with the solar value. By contrast, N is *enhanced* in the hotter sdO stars, by factors reaching  $\sim 100$ .

Perhaps the most remarkable abundance behavior in that group of hydrogen-rich subdwarfs is that of Si. BKSS and BHS had already noted a large deficiency of silicon in HD 149382 and Feige 66, two hot sdOB stars. Similar results are obtained here for the two hottest stars in our sample: in the range between 30,000 K and 40,000 K, the silicon abundance remains below  $10^{-5}$  the solar value. At the hot end, the situation is complicated—once again—by the fact that LB 3459 and Feige 110, of similar temperature, have silicon abundance that differ by  $\gtrsim 3.0$  dex. Of note, however, is the fact that silicon is overabundant ( $\lesssim 1.0$  dex) in the still hotter O subdwarfs. At the cool end, Feige 65 is also underabundant in silicon, but only by a factor  $\sim 10^2$ . The relatively larger Si abundance observed in that cooler sdB star is substantiated by the solar silicon abundances determined (HD 4539) or inferred (HD 205805) in the cruder analyses of the optical spectra of two other cool sdB stars (Baschek, Sargent, and Searle 1972; Baschek and Norris 1970). BHS also quoted preliminary analyses of high-dispersion *IUE* data of these two stars (e.g., Baschek, Kud-

ritzki, and Scholz 1980) which confirm the approximately solar silicon abundances of these two objects. Furthermore, Heber *et al.* (1984b) also argue for nearly solar silicon abundances in their sample of six B subdwarfs below 30,000 K, on the basis of the presence of silicon features in low-dispersion *IUE* images.

Downward diffusion of helium is now recognized as the most likely causes of the helium deficiency observed in the hot B and OB subdwarfs (Greenstein and Sargent 1974; Baschek and Norris 1975; Winget and Cabot 1980; Kudritzki *et al.* 1982; Wesemael *et al.* 1982). It thus seems natural to call on similar processes to explain the patterns of heavy-element abundances summarized above, as has already been done by BKSS, BHS, and Heber *et al.* (1984a, b). However, while diffusion time scales for helium in subdwarf envelopes have been presented by Winget and Cabot (1980) and Wesemael *et al.* (1982), the diffusion time scales of heavier elements in the atmospheres of hydrogen-rich subdwarfs have—to our knowledge—never been estimated.

To remedy this situation, we have calculated diffusion time scales for C, N, and Si in the atmospheres of Feige 65 and Ton S-227; we follow the method of Fontaine and Michaud (1979), in which have been incorporated the improved diffusion coefficients of Paquette (1983). Only thermal diffusion and gravitational settling are taken into account.

As might have been anticipated for these intermediate-gravity objects, the downward diffusion time scales are all relatively short. We find  $\tau_C = 2.6 \times 10^3$  yr,  $\tau_N = 2.1 \times 10^3$  yr, and  $\tau_{Si} = 1.7 \times 10^3$  yr near  $\tau_{Ross} = 10$  in Feige 65; in Ton S-227,  $\tau_C = 3.7 \times 10^2$  yr,  $\tau_N = 2.4 \times 10^2$  yr, and  $\tau_{Si} = 1.8 \times 10^2$  yr. Although the evolutionary time scales of sdB and sdOB stars are unknown, they are likely to be (much?) longer than the diffusion time scales estimated here.

The short settling time scales of heavy elements imply that physical mechanisms disrupting the diffusion process must be considered to explain the residual metal abundance observed. Radiative element support has already been suggested in this context (BKSS, BHS, Heber *et al.* 1984a, b), and the plausibility of that suggestion is strengthened by the results of Michaud, Vauclair, and Vauclair (1983) for their hottest (least massive) horizontal-branch model; at  $T_e = 20,700$  K,  $\log g = 5.2$ , that model is cooler than, e.g., Feige 65, but of comparable surface gravity. Already at that temperature, selective radiative accelerations are found to be significant (i.e.,  $g_R \gtrsim g$ ) in determining the eventual atmospheric abundance. Their relative importance will increase further as one considers even hotter objects. Within this framework, BKSS and BHS have already suggested that the large underabundances of silicon observed between 30,000 and 40,000 K (see Fig. 6) are associated with the noble gas configuration assumed by silicon in the atmosphere. Indeed, in main-sequence and horizontal-branch stars, the predicted abundance anomalies are known to be strongly modulated by these configurations (Michaud *et al.* 1976; Michaud, Vauclair, and Vauclair 1983). However, only detailed calculations of radiative forces can show if the radiative acceleration, properly averaged over the ionization states, can dip sufficiently below its gravitational (and thermal) counterpart to account for the large ( $\gtrsim 5$  dex) underabundances observed. This problem is considered elsewhere (Michaud *et al.* 1985).

If radiative forces assume the importance suggested here in the atmospheres of hot subdwarfs, the straightforward interpretation of the observed abundances in terms of ashes of nuclear processes (such as the CNO cycle; Gruschinske *et al.*

1980; Simon *et al.* 1980; Heber *et al.* 1984a) appears seriously hampered, if not outright impossible. Furthermore, it should be kept in mind that extremely little is known about other potential mechanisms that could hinder diffusion in hot sub-dwarfs. More exotic disruptive agents, such as meridional circulation, turbulent motions, and even a modest mass outflow, should perhaps not be dismissed too facilely in these stars.

We are grateful to F. K. Bruhweiler for some pertinent comments at the early stages of this work, and to P. Bergeron and G. Michaud for several discussions on this topic. We are also

indebted to the KPNO and *IUE* staffs for their help in the acquisition and retrieval of our data, to the director of KPNO for the continuing support of our observing program there, and to the Astronomical Data Center at the NASA/Goddard Space Flight Center for providing archived *IUE* images. This work was supported in part by the NSERC Canada, by the NASA grant NAG 5-343, and by the NSF grants AST 81-17177 and AST 83-14788 to Arizona State University. Computing funds for this project were kindly made available by the Centre de Calcul of the Université de Montréal.

## REFERENCES

- Baschek, B., Höfflich, P., and Scholz, M. 1982, *Astr. Ap.*, **112**, 76 (BHS).  
 Baschek, B., Kudritzki, R. P., and Scholz, M. 1980, in *Proc. 2d European IUE Conf.* (EAS SP-157), p. 319.  
 Baschek, B., Kudritzki, R. P., Scholz, M., and Simon, K. P. 1982, *Astr. Ap.*, **108**, 387 (BKSS).  
 Baschek, B., and Norris, J. 1970, *Ap. J. Suppl.*, **19**, 327.  
 ———. 1975, *Ap. J.*, **199**, 694.  
 Bergeron, P., Fontaine, G., Lacombe, P., Wesemael, F., Crawford, D. L., and Jakobsen, A. M. 1984, *A.J.*, **89**, 374.  
 Bianchi, L., and Bohlin, R. C., 1984, *Astr. Ap.*, **134**, 31.  
 Bruhweiler, F. C. 1984, in *Future of Ultraviolet Astronomy Based on Six Years of IUE Research* (NASA CP-2349), p. 269.  
 Bruhweiler, F. C., and Dean, C. A. 1983, *Ap. J. (Letters)*, **274**, L87.  
 Bruhweiler, F. C., and Kondo, Y. 1982, *Ap. J.*, **259**, 232.  
 Bruhweiler, F. C., Kondo, Y., and McCluskey, G. E. 1981, *Ap. J. Suppl.*, **46**, 255.  
 Dufton, P. L., Durrant, A. C., and Durrant, C. J. 1981, *Astr. Ap.*, **97**, 10.  
 Fontaine, G., and Michaud, G. 1979, *Ap. J.*, **231**, 826.  
 Giddings, J. R., and Dworetzky, M. M. 1978, *M.N.R.A.S.*, **183**, 265.  
 Graham, J. A., and Slettebak, A. 1973, *A.J.*, **78**, 295.  
 Greenstein, J. L., and Sargent, A. I. 1974, *Ap. J. Suppl.*, **28**, 157.  
 Grunschinske, J., Hunger, K., Kudritzki, R. P., and Simon, K. P. 1980, in *Proc. 2d European IUE Conf.* (ESA SP-157), p. 311.  
 Hamann, W.-R., Grunschinske, J., Kudritzki, R. P., and Simon, K. P. 1981, *Astr. Ap.*, **104**, 249.  
 Heber, U., Hamann, W.-R., Hunger, K., Kudritzki, R. P., Simon, K. P., and Méndez, R. H. 1984a, *Astr. Ap.*, **136**, 331.  
 Heber, U., Hunger, K., Jonas, G., and Kudritzki, R. P. 1984b, *Astr. Ap.*, **130**, 119.  
 Henry, R. B. C., Shipman, H. L., and Wesemael, F. 1985, *Ap. J. Suppl.*, **57**, 145.  
 Kelly, R. L., and Palumbo, L. J. 1973, *Atomic and Ionic Emission below 2000 Å* (Washington: NRL Rept. 7599).  
 Kudritzki, R. P., Simon, K. P., Lynas-Gray, A. E., Kilkenny, D., and Hill, P. W. 1982, *Astr. Ap.*, **106**, 254.  
 Kurucz, R. L. 1979, *Ap. J. Suppl.*, **40**, 1.  
 Lynas-Gray, A. E., Heber, U., Kudritzki, R. P., and Simon, K. P. 1984, in *Proc. 4th European IUE Conf.* (ESA SP-218), p. 285.  
 Michaud, G., Bergeron, P., Wesemael, F., and Fontaine, G. 1985, *Ap. J.*, **299**, in press.  
 Michaud, G., Charland, Y., Vauclair, S., and Vauclair, G. 1976, *Ap. J.*, **210**, 447.  
 Michaud, G., Vauclair, G., and Vauclair, S. 1983, *Ap. J.*, **267**, 256.  
 Paquette, C. 1983, M.Sc. thesis, Université de Montréal.  
 Poulizac, M. C., Druetta, M., and Ceyzériat, P. 1971, *J. Quant. Spectrosc. Rad. Transf.*, **11**, 1087.  
 Rossi, L., Viotti, R., and Altamore, A. 1984, *Astr. Ap. Suppl.*, **55**, 361.  
 Sahal-Bréchet, S., and Segre, E. R. A. 1971, *Astr. Ap.*, **13**, 161.  
 Simon, K. P., Grunschinske, J., Hunger, K., and Kudritzki, R. P. 1980, in *Proc. 2d European IUE Conf.* (ESA SP-157) p. 305.  
 Wesemael, F., Auer, L. H., Van Horn, H. M., and Savedoff, M. P. 1980, *Ap. J. Suppl.*, **43**, 159.  
 Wesemael, F., Holberg, J. B., Veilleux, S., Lamontagne, R., and Fontaine, G. 1985, *Ap. J.*, **298**, 859.  
 Wesemael, F., Winget, D. E., Cabot, W., Van Horn, H. M., and Fontaine, G. 1982, *Ap. J.*, **254**, 221.  
 Wiese, W. L., Smith, M. W., and Glennon, B. M. 1966, *Atomic Transition Probabilities*, Vol. 1 (NSRDS-NBS4).  
 Winget, D. E., and Cabot, W. 1980, *Ap. J.*, **242**, 1166.

G. FONTAINE, R. LAMONTAGNE, and F. WESEMAEL: Département de Physique, Université de Montréal, C.P. 6128, Succ. A, Montréal, Québec H3C 3J7, Canada

E. M. SION: Department of Astronomy, Villanova University, Villanova, PA 19085